molecular pharmaceutics

Article

pubs.acs.org/molecularpharmaceutics

Comparison of Two Site-Specifically ^{18}F-Labeled Affibodies for PET Imaging of EGFR Positive Tumors

Xinhui Su,[†,‡] Kai Cheng,[‡] Jongho Jeon,[‡,⊥] Bin Shen,[‡] Gianina Teribele Venturin,[‡,§] Xiang Hu,[‡] Jianghong Rao,[‡] Frederick T. Chin,[‡] Hua Wu,[∥] and Zhen Cheng*[,‡]

[†]Department of Nuclear Medicine, Zhongshan Hospital Xiamen University, Xiamen 361004, China

[‡]Molecular Imaging Program at Stanford (MIPS), Department of Radiology, Bio-X Program, and Stanford Cancer Center, Stanford University School of Medicine, Stanford, California 94305, United States

[⊥]Research Division for Biotechnology, Advanced Radiation Technology Institute, Korea Atomic Energy Research Institute, 29 Geumgu-gil, Jeongeup-si, Jeonbuk 580-185, Republic of Korea

[§]Instituto do Cérebro do Rio Grande do Sul (InsCer), Universidade Católica do Rio Grande do Sul (PUCRS), Porto Alegre, Brazil

[∥]Department of Nuclear Medicine, The First Affiliated Hospital of Xiamen University, Xiamen 361003, China

ABSTRACT: The epidermal growth factor receptor (EGFR) serves as an attractive target for cancer molecular imaging and therapy. Our previous positron emission tomography (PET) studies showed that the EGFR-targeting affibody molecules ^{64}Cu-DOTA-$Z_{EGFR:1907}$ and ^{18}F-FBEM-$Z_{EGFR:1907}$ can discriminate between high and low EGFR-expression tumors and have the potential for patient selection for EGFR-targeted therapy. Compared with ^{64}Cu, ^{18}F may improve imaging of EGFR-expression and is more suitable for clinical application, but the labeling reaction of ^{18}F-FBEM-$Z_{EGFR:1907}$ requires a long synthesis time. The aim of the present study is to develop a new generation of ^{18}F labeled affibody probes (Al^{18}F-NOTA-$Z_{EGFR:1907}$ and ^{18}F-CBT-$Z_{EGFR:1907}$) and to determine whether they are suitable agents for imaging of EGFR expression. The first approach consisted of conjugating $Z_{EGFR:1907}$ with NOTA and radiolabeling with Al^{18}F to produce Al^{18}F-NOTA-$Z_{EGFR:1907}$. In a second approach the prosthetic group ^{18}F-labeled-2-cyanobenzothiazole (^{18}F-CBT) was conjugated to Cys-$Z_{EGFR:1907}$ to produce ^{18}F-CBT-$Z_{EGFR:1907}$. Binding affinity and specificity of Al^{18}F-NOTA-$Z_{EGFR:1907}$ and ^{18}F-CBT-$Z_{EGFR:1907}$ to EGFR were evaluated using A431 cells. Biodistribution and PET studies were conducted on mice bearing A431 xenografts after injection of Al^{18}F-NOTA-$Z_{EGFR:1907}$ or ^{18}F-CBT-$Z_{EGFR:1907}$ with or without coinjection of unlabeled affibody proteins. The radiosyntheses of Al^{18}F-NOTA-$Z_{EGFR:1907}$ and ^{18}F-CBT-$Z_{EGFR:1907}$ were completed successfully within 40 and 120 min with a decay-corrected yield of 15% and 41% using a 2-step, 1-pot reaction and 2-step, 2-pot reaction, respectively. Both probes bound to EGFR with low nanomolar affinity in A431 cells. Although ^{18}F-CBT-$Z_{EGFR:1907}$ showed instability *in vivo*, biodistribution studies revealed rapid and high tumor accumulation and quick clearance from normal tissues except the bones. In contrast, Al^{18}F-NOTA-$Z_{EGFR:1907}$ demonstrated high *in vitro* and *in vivo* stability, high tumor uptake, and relative low uptake in most of the normal organs except the liver and kidneys at 3 h after injection. The specificity of both probes for A431 tumors was confirmed by their lower uptake on coinjection of unlabeled affibody. PET studies showed that Al^{18}F-NOTA-$Z_{EGFR:1907}$ and ^{18}F-CBT-$Z_{EGFR:1907}$ could clearly identify EGFR positive tumors with good contrast. Two strategies for ^{18}F-labeling of affibody molecules were successfully developed as two model platforms using NOTA or CBT coupling to affibody molecules that contain an N-terminal cysteine. Al^{18}F-NOTA-$Z_{EGFR:1907}$ and ^{18}F-CBT-$Z_{EGFR:1907}$ can be reliably obtained in a relatively short time. Biodistribution and PET studies demonstrated that Al^{18}F-NOTA-$Z_{EGFR:1907}$ is a promising PET probe for imaging EGFR expression in living mice.

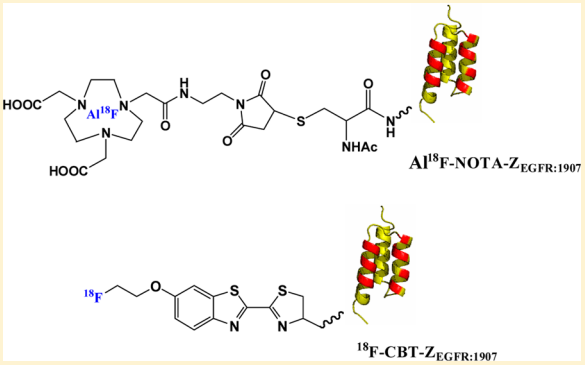

KEYWORDS: *affibody, EGFR, PET, ^{18}F, NOTA, CBT*

INTRODUCTION

The epidermal growth factor receptor (EGFR) plays an important role in neoplastic processes of cell proliferation, inhibition of apoptosis, angiogenesis, and metastatic spread.[1] Overexpression of EGFR in tumors has been associated with resistance against conventional drug treatment and radiation and may predict poor prognosis.[2−4] Detection of EGFR expression by molecular imaging could be a useful tool for evaluation of antitumor drug

Special Issue: Positron Emission Tomography: State of the Art

Received: April 24, 2014
Revised: June 21, 2014
Accepted: June 27, 2014
Published: June 27, 2014

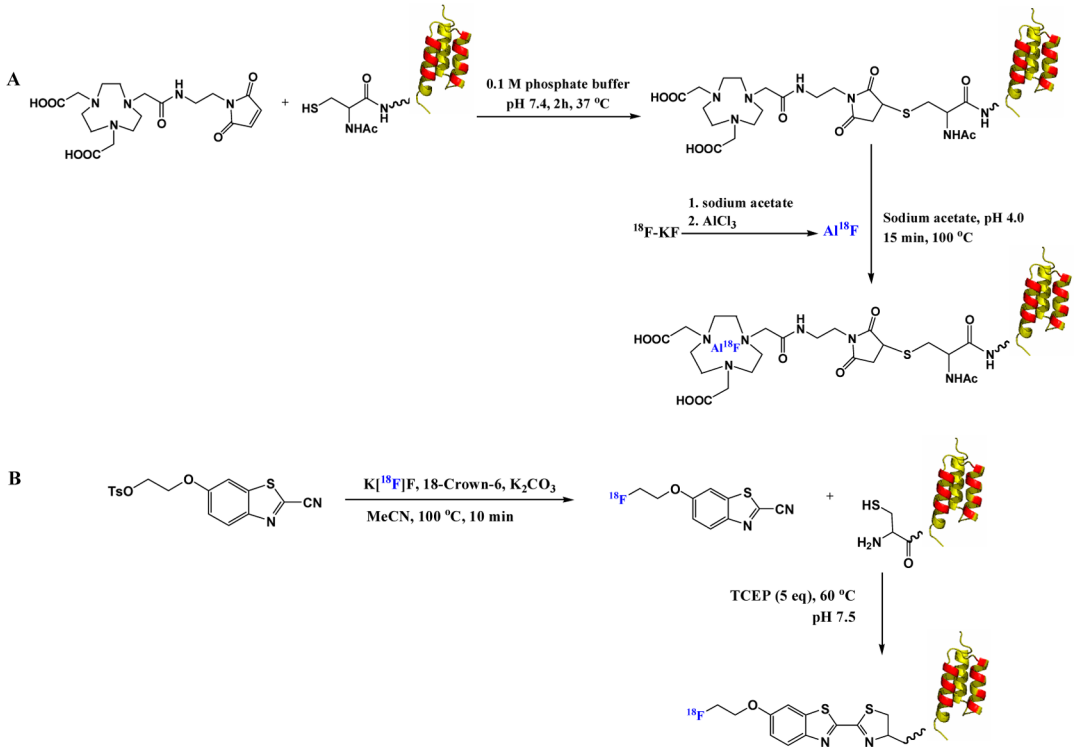

Figure 1. Schemes of radiosynthesis of Al^{18}F-NOTA-$Z_{EGFR:1907}$ and ^{18}F-CBT-$Z_{EGFR:1907}$.

effect, stratification of cancer patients for molecularly targeted therapy, and prognosis of cancer patients, as it could provide real time data with fewer false-negative results.[5]

Affibody molecules are based on a 58 amino acid residue protein domain, derived from one of the IgG-binding domains of staphylococcal protein A, and has been engineered to be chemically stable and to bind target proteins with high affinity.[6,7] Because of their small size (~7 kDa) and high affinity, affibody molecules generally show fast and good tumor tissue penetration and accumulation, and rapid clearance from the blood, resulting in high imaging contrast within a short period (for example, 0.5−1 h) after injection. Antihuman epidermal growth factor receptor 2 (HER2) affibody molecules (Z_{HER2}) and their derivatives have been radiolabeled with various radionuclides for imaging of tumors overexpressing HER2 in animal models.[7−10] Subsequently, ^{111}In- or ^{68}Ga-labeled Z_{HER2} have been successfully and safely used to visualize HER2-expressing tumors in patients with metastatic breast cancer. These clinical studies clearly demonstrate that affibody molecules have great potential to become a promising new class of cancer-targeting ligands for clinical translation.[11] Overall the previous preclinical and clinical studies encourage us to further develop clinical translatable affibody probes to image other tumor targets such as EGFR.[12,13]

We have previously reported the site-specific coupling of an anti-EGFR affibody molecule ($Z_{EGFR:1907}$) with maleimido-monoamide-DOTA (MMA-DOTA, 1,4,7,10-tetraazacyclododecane-1,4,7-trisaceticacid-10-maleimidoethylmonoamide) to produce the bioconjugate, DOTA-$Z_{EGFR:1907}$, that was radiolabeled with ^{64}Cu.[13] This conjugate allowed high-contrast imaging of EGFR-expressing xenografts. However, imaging of EGFR expression with affibody molecules and further clinical translation of them can be further improved by ^{18}F-labeling. Not only are ^{18}F probes more clinically relevant than ^{64}Cu but also they have good imaging characteristics and a suitable half-life for relatively low molecular weight proteins and peptides. Therefore, we recently radiolabeled $Z_{EGFR:1907}$ with *N*-2-(4-^{18}F-fluorobenzamido)-ethyl maleimide (^{18}F-FBEM) to produce the positron emission tomography (PET) probe, ^{18}F-FBEM-$Z_{EGFR:1907}$, for imaging EGFR expression in a variety of tumor models.[12] Although ^{18}F-FBEM-$Z_{EGFR:1907}$ PET allowed us to visualize EGFR-expressing tumors, the labeling procedure to obtain the probe is complex and tedious, and requires a long radiosynthesis time (4-step radiosynthesis, 3 h, 10% decay corrected yield), which severely limits further applications of ^{18}F-FBEM-$Z_{EGFR:1907}$.

Recently, two new and simple methods for labeling of biomolecules with ^{18}F have been developed. In the first one, peptides conjugated to MMA-NOTA (1,4,7-triazacyclononane-*N*,*N*′,*N*″-triacetic acid maleimidoethylmonoamide) and its analogues have been labeled with ^{18}F via the formation of aluminum ^{18}F-fluoride (Al^{18}F) and its complexation by NOTA directly (one step radiosynthesis).[14,15] The second method involves ^{18}F-labeling of N-terminal cysteine-bearing peptides and proteins and is based on a rapid condensation reaction between ^{18}F-fluorinated-2-cyanobenzothiazole (^{18}F-CBT) and cysteine (2-step reaction).[16] Both methods allow rapid and efficient labeling of peptides and proteins with ^{18}F. Al^{18}F-NOTA in particular has been applied to label many peptides including RGD and anti-HER2 affibody molecules.[17,18] The Al^{18}F-NOTA labeled RGD peptides have also been successfully used for PET imaging of a lung cancer patient recently.[19]

Our ultimate goal is to translate an ^{18}F-labeled Z_{EGFR} into clinical applications. Therefore, in the current study, we aimed to use the above radiofluorination strategies (Al^{18}F-NOTA and ^{18}F-CBT) to site-specifically label $Z_{EGFR:1907}$ and further determine whether the resulting PET probes, Al^{18}F-NOTA-$Z_{EGFR:1907}$ and ^{18}F-CBT-$Z_{EGFR:1907}$, are suitable agents for imaging mice bearing EGFR expressing A431 tumors. For this purpose, NOTA-conjugated $Z_{EGFR:1907}$ was prepared and radiolabeled with ^{18}F to produce Al^{18}F-NOTA-$Z_{EGFR:1907}$, and the prosthetic group (^{18}F-CBT) was conjugated to Cys-$Z_{EGFR:1907}$ to produce ^{18}F-CBT-$Z_{EGFR:1907}$ (Figure 1). The *in vitro* properties and *in vivo*

dx.doi.org/10.1021/mp5003043 | *Mol. Pharmaceutics* 2014, 11, 3947−3956

performance of $Al^{18}F$-NOTA-$Z_{EGFR:1907}$ were then compared with those of ^{18}F-CBT-$Z_{EGFR:1907}$ in A431 cells and tumor xenografts.

MATERIALS AND METHODS

General. MMA-NOTA was purchased from CheMatech Inc. (Dijon, France). Phosphate-buffered saline (PBS), high-glucose Dulbecco's modified eagle medium (DMEM), 10% fetal bovine serum (FBS), 1% penicillin−streptomycin, 0.1% trypsin, trypsin−EDTA, and TrypLE-Express were purchased from Invitrogen Life Technologies (Carlsbad, California). Dimethyl sulfoxide (DMSO) and acetonitrile (MeCN) were purchased from Fisher Scientific (Pittsburgh, Pennsylvania). Dimethylformamide (DMF), trifluoroacetic acid (TFA), thioanisole (TIS), ethanedithiol (EDT), ethylene-diamine-tetra-acetic acid (EDTA), tris(2-carboxyethyl)-phosphine hydrochloride (TCEP HCl), *N*,*N*-diisopropyl-ethylamine (DIPEA), ethyl acetate, dithiothreitol (DTT), mouse serum, and all other standard synthesis reagents were purchased from Sigma-Aldrich Chemical Co. (St. Louis, Missouri). All chemicals were used without further purification.

The affibody molecules Ac-Cys-$Z_{EGFR:1907}$ (Ac-CVDNKFNKEMWAAWEEIRNLPNLNGWQMTAFIASLVDDPSQSANLLAEAKKLNDAQAPK-NH_2) and Cys-$Z_{EGFR:1907}$ (CVDNKFNKEMWAAWEEIRNLPNLNGWQMTAFIASLVDDPSQSANLLAEAKKLNDAQAPK-NH_2) were synthesized on a CS Bio CS336 instrument (CS Bio Company, Menlo Park, California) in our laboratory as previously described.[13] The purified peptide was dissolved in water, and the concentration was determined by amino acid analysis (Molecular Structure Facility, University of California, Davis, CA). Peptide purity and molecular mass were determined by analytic scale reversed-phase high-performance liquid chromatography (RP-HPLC, model: 3000 HPLC System, Dionex Corporation, Sunnyvale, California) and matrix-assisted laser desorption/ionization−time-of-flight mass spectrometry (MALDI-TOF-MS, model: Perseptive Voyager-DE RP Biospectrometer, Framinghan, Massachusetts) or electrospray ionization mass spectrometry (ESI-MS, model: Micromass ZQ single quadrupole LC−MS, Milford, Massachusetts) as previously described.[13] The human epidermoid carcinoma cancer cell line A431 was obtained from the American Type Tissue Culture Collection (Manassas, Virginia). Female nude mice were purchased from Charles River Laboratories (Boston, Massachusetts).

Radiosynthesis of $Al^{18}F$-NOTA-$Z_{EGFR:1907}$. The affibody molecule NOTA-$Z_{EGFR:1907}$ was radiolabeled with ^{18}F according to a previously reported method[14,15,18] (Figure 1A). First, Ac-Cys-$Z_{EGFR:1907}$ was conjugated with the bifunctional chelator MMA-NOTA using the method described below: Ac-Cys-$Z_{EGFR:1907}$ was dissolved in freshly degassed phosphate buffer (0.1 M, pH 7.4) at a concentration of 1 mg/mL. Twenty equivalents of MMA-NOTA dissolved in DMSO (10 mM) were added. After mixing by vortexing for 2 h, the product was purified by RP-HPLC with a protein-and-peptide C4 column (Grace Vydac 214TP54, Columbia, Maryland) using a gradient system of solvent A (0.1% TFA/H_2O) and solvent B (0.1%TFA/MeCN). The flow rate was 4 mL/min, with the mobile phase starting from 90% solvent A and 10% solvent B (0−3 min) to 35% solvent A and 65% solvent B at 33 min. Fractions containing the product were collected and lyophilized. The identity of the products was confirmed by MALDI-TOF-MS.

Second, nonradioactive $Al^{19}F$-NOTA-$Z_{EGFR:1907}$, a reference standard, was synthesized with NOTA-$Z_{EGFR:1907}$ and $K^{19}F$. To a solution of KF (2 mM, 5 μL) in 20 μL of sodium acetate buffer (0.1 M, pH 4) was added $AlCl_3$ (2 mM, 5 μL). Then, NOTA-$Z_{EGFR:1907}$ (50 μg) dissolved in 50 μL of sodium acetate buffer (0.1 M, pH 4) was added, and the reaction mixture was incubated for 15 min at 100 °C. The resulting conjugate, $Al^{19}F$-NOTA-$Z_{EGFR:1907}$ was purified by HPLC.

Lastly, ^{18}F radiolabeling of NOTA-$Z_{EGFR:1907}$ was performed. ^{18}F-fluoride (37×10^3 MBq) was prepared by proton bombardment of 2.5 mL of [^{18}O] enriched water target via the ^{18}O (p, n) ^{18}F nuclear reaction. The ^{18}F-fluoride was then trapped onto a Sep-Pak QMA cartridge (Waters, Milford, Massachusetts), washed with 3 mL of metal-free water, and eluted from the cartridge with 100 μL of 0.9% NaCl. $Al^{18}F$ was prepared by adding $AlCl_3$ (2 mM, 2 μL) in sodium acetate buffer (0.1 M, pH 4). NOTA-$Z_{EGFR:1907}$ (150 μg) was dissolved in 25 μL of sodium acetate buffer (0.5 M, pH 4). To the dissolved affibody molecule, acetonitrile (25 μL) and $Al^{18}F$ (50 μL, $1.3-1.6 \times 10^3$ MBq) were added, then the reaction mixture was incubated for 15 min at 100 °C. An Oasis HLB cartridge (30 mg; Waters) was used to remove unincorporated $Al^{18}F$, and the desired product was purified with HPLC using the same elution gradient described for NOTA-$Z_{EGFR:1907}$ purification. The HPLC fractions containing $Al^{18}F$-NOTA-$Z_{EGFR:1907}$ were collected, combined, and evaporated. $Al^{18}F$-NOTA-$Z_{EGFR:1907}$ was reconstituted in PBS (0.1 M, pH 7.4) and passed through a 0.22 μm Millipore filter into a sterile vial for *in vitro* and animal experiments.

Radiosynthesis of ^{18}F-CBT-$Z_{EGFR:1907}$. Nonradioactive ^{19}F-CBT-$Z_{EGFR:1907}$ was used as a reference for characterization of ^{18}F-CBT-$Z_{EGFR:1907}$ and prepared by reaction of Cys-$Z_{EGFR:1907}$ with ^{19}F-CBT. Briefly, TCEP HCl solution (2.4 μL, 10 mM) and DIPEA (360 nmol) were added to Cys-$Z_{EGFR:1907}$ solution (30 μL, 200 μM in DMF) and then the resulting solution was mixed with ^{19}F-CBT solution (1.8 μL, 10 mM, 3 equiv). The resulting mixture was heated to 60 °C for 1 h. The crude product was purified with semipreparative HPLC using Phenomenex Gemini column (10 mm × 250 mm, 5 μm) using a linear gradient from deionized water with 0.1% TFA to MeCN with 0.1% TFA: 0−3 min 0−40% (MeCN); 3−35 min 40−100% (MeCN); and the flow rate was 3 mL/min.

Cys-$Z_{EGFR:19077}$ was labeled with ^{18}F-CBT according to the procedure we recently described[16] (Figure 1B). First, ^{18}F-labeling of tosylated CBT was performed. 18-Crown-6/K_2CO_3 solution (1 mL, 15:1 MeCN/H_2O, 16.9 mg of 18-Crown-6 and 4.4 mg of K_2CO_3) was used to elute the activity of ^{18}F-fluoride from QMA cartridge into a dried glass reactor. The resulting solution was azeotropically dried with sequential MeCN evaporations at 90 °C. A solution of [2-((2-cyanobenzo[*d*]thiazol-6-yl)-oxy)ethyl 4-methylbenzenesulfonate] (2 mg in 1 mL of anhydrous MeCN) was added to the reactor, and the mixture heated at 90 °C for 10 min. After cooling to 30 °C, HCl (0.05 M, 2.5 mL) was added to quench the reaction and prevent basic hydrolysis of the product ^{18}F-CBT. The crude mixture was then purified with a semipreparative HPLC using the same elution gradient described for ^{19}F-CBT purification. The collected ^{18}F-CBT solution was diluted with H_2O (20 mL) and passed through a C18 cartridge. The trapped ^{18}F-CBT was eluted out from the cartridge with Et_2O (2.5 mL), and the Et_2O was removed by a helium stream. The isolated radiochemical yield of ^{18}F-CBT was ca. 20% ($5.18-5.55 \times 10^3$ MBq, decay-corrected to end of bombardment). For the radiosynthesis of ^{18}F-CBT-$Z_{EGFR:1907}$, Cys-$Z_{EGFR:1907}$ (150 μg, 7.5 nmol) was dissolved in PBS buffer (0.1 M, pH 7.4) containing 5 equiv of TCEP HCl and 50 equiv of $NaHCO_3$. The resulting solution was added to ^{18}F-CBT (1.85×10^3 MBq) in DMF (200 μL) at 60 °C. After 20 min, the reaction was quenched with 5% AcOH aqueous solution. The crude product was purified with a semipreparative HPLC using Phenomenex Gemini column

dx.doi.org/10.1021/mp5003043 | *Mol. Pharmaceutics* 2014, 11, 3947−3956

(10 mm × 250 mm, 5 μm) using a linear gradient from deionized water with 0.1% TFA to MeCN with 0.1% TFA: 0−5 min 0−5% (MeCN); 5−42 min 5−65% (MeCN); and the flow rate was 5 mL/min.

Cell Assays. Cell uptake and receptor saturation assays were performed as previously described with minor modifications.[13] Briefly, the EGFR positive A431 cell line was cultured in high glucose DMEM supplemented with 10% fetal bovine serum (FBS) and 1% penicillin−streptomycin. The cells were maintained in a humidified atmosphere of 5% CO_2 at 37 °C, with the medium changed every 2 days. A 70−80% confluent monolayer was detached by 0.1% trypsin and dissociated into a single cell suspension for further cell culture.

Cell Uptake Assays. The A431 cells were washed three times with PBS and dissociated with 0.25% trypsin−EDTA. DMEM medium was then added to neutralize trypsin−EDTA. Cells were spun down and resuspended with serum-free DMEM. Cells (0.5×10^6) were incubated at 37 °C for 0.25 to 2 h with 7.4×10^{-3} MBq Al^{18}F-NOTA-$Z_{EGFR:1907}$ or ^{18}F-CBT-$Z_{EGFR:1907}$ in 0.5 mL of serum-free DMEM medium. The nonspecific binding of Al^{18}F-NOTA-$Z_{EGFR:1907}$ or ^{18}F-CBT-$Z_{EGFR:1907}$ with A431 cells was determined by coincubation with 0.6 μM nonradiolabeled NOTA-$Z_{EGFR:1907}$ or Cys-$Z_{EGFR:1907}$. The cells were washed three times with 0.01 M PBS (pH 7.4) at room temperature. Cell were then washed three times with chilled PBS and spun down at a speed of 7000−8000 rpm. The cell pellets at the bottom of the tube were spliced, and the radioactivity of the pellets was measured using a γ-counter (PerkinElmer 1470, Waltham, Massachusetts). The uptake (counts/min) was normalized to the percentage of binding for analysis using Excel (Microsoft Software Inc., Redmond, Washington).

Receptor Saturation Assays. A431 cells (0.3×10^6) were plated on 6-well plates 1 day before the experiment. Cells were washed with PBS three times. Serum-free DMEM (1 mL) was added to each well, followed by the addition of either Al^{18}F-NOTA-$Z_{EGFR:1907}$ ($8.9−532.8 \times 10^{-3}$ MBq, 2−120 nM final concentration) or ^{18}F-CBT-$Z_{EGFR:1907}$ ($8.9−532.8 \times 10^{-3}$ MBq, 2−120 nM final concentration). The nonspecific binding of Al^{18}F-NOTA-$Z_{EGFR:1907}$ or ^{18}F-CBT-$Z_{EGFR:1907}$ with A431 cells was determined by coincubation with 100 times excess of NOTA-$Z_{EGFR:1907}$ or Cys-$Z_{EGFR:1907}$. The plates were then put on ice for 2 h, and the cells were washed with cold PBS three times and detached with TrypLE-Express. The radioactivity of the cells was measured using a γ-counter. Specific binding (SB) = total binding (TB) − nonspecific binding (NSB). The data were analyzed using GraphPad Prism (GraphPad Software, Inc., San Diego, California), and the dissociation constant (K_D value) of ^{18}F-NOTA-$Z_{EGFR:1907}$ and ^{18}F-CBT-$Z_{EGFR:1907}$ were calculated from a 1-site-fit binding curve.

***In Vitro* and *In Vivo* Stability.** *In vitro and in vivo* stability were determined similarly to the procedures previously described with minor modifications.[12,13]

In Vitro Serum Stability Assay. Al^{18}F-NOTA-$Z_{EGFR:1907}$ (1.5−6.7 MBq) or ^{18}F-CBT-$Z_{EGFR:1907}$ (2.2−7.4 MBq) was incubated in 0.5 mL of mouse serum for 1 and 2 h at 37 °C. At each time point, the mixture was precipitated with 300 μL of ethanol and centrifuged at 16,000*g* for 2 min. The supernatant was transferred to a new Eppendrof tube, and DMF (300 μL) was added to precipitate the residue of serum protein. After centrifugation, the supernatant was acidified with 300 μL of buffer A (water + 0.1% TFA) and filtered using a 0.2 μm nylon Spin-X column (Corning Inc. Corning, New York). The filtrates were then analyzed by radio-HPLC under conditions identical to the ones used to analyze the original radiolabeled compound. The percentage of intact Al^{18}F-NOTA-$Z_{EGFR:1907}$ and ^{18}F-CBT-$Z_{EGFR:1907}$ were determined by quantifying peaks corresponding to the intact and the degradation products.

In Vivo Stability Assay. Two groups of A431 mice (for each group n = 3) were injected with Al^{18}F-NOTA-$Z_{EGFR:1907}$ (5.8 MBq) or ^{18}F-CBT-$Z_{EGFR:1907}$ (7.4 MBq) via a tail vein and euthanized at 1 h after injection. The tumors were removed and homogenized with DMF (0.5 mL) with 1% Triton X-100 (Sigma-Aldrich). Blood samples were centrifuged immediately after collection to remove the blood cells. The plasma portions were added to DMF (0.5 mL) with 1% Triton X-100. After centrifugation, the supernatant portions were diluted with solution A (99.9% H_2O with 0.1% TFA) and centrifuged again at 16,000*g* for 2 min with a nylon filter. The filtrates were analyzed by radio-HPLC under conditions identical to those used for analyzing the original radiolabeled peptide.

Biodistribution Studies. The animal procedures were performed according to a protocol approved by the Stanford University Institutional Animal Care and Use Committee. Approximately 5×10^6 cultured A431 cells suspended in PBS were implanted subcutaneously in the right upper or lower shoulders of nude mice. Tumors were allowed to grow to around 0.5−1.0 cm in diameter (10−15 days) and then the tumor-bearing mice underwent *in vivo* biodistribution and imaging studies.

For biodistribution studies, A431 tumor-bearing mice (for each group n = 4) were injected with ^{18}F-NOTA-$Z_{EGFR:1907}$ (1.9−2.6 MBq) or ^{18}F-CBT-$Z_{EGFR:1907}$ (1.48−2.22 MBq) with 30 μg of nonradioactive Ac-Cys-$Z_{EGFR:1907}$ or Cys-$Z_{EGFR:1907}$, respectively, through a tail vein. At 3 h after injection, the mice were sacrificed, and tumors and normal tissues of interest were removed and weighed, and their radioactivity was measured in a γ-counter. The radioactivity uptake in the tumor and normal tissues was expressed as a percentage of the injected radioactivity per gram of tissue (%ID/g). In order to study the *in vivo* EGFR targeting specificity of Al^{18}F-NOTA-$Z_{EGFR:1907}$ and ^{18}F-CBT-$Z_{EGFR:1907}$, unlabeled Ac-Cys-$Z_{EGFR:1907}$ or Cys-$Z_{EGFR:1907}$ protein (300 μg) was coinjected with the corresponding ^{18}F-labeled $Z_{EGFR:1907}$ in nude mice bearing A431 tumors (n = 4) via a tail vein, and biodistribution studies were conducted at 3 h after injection.

Small-Animal PET Imaging. PET imaging of tumor-bearing mice was performed on a microPET R4 rodent model scanner (Siemens Medical Solutions USA, Inc., Malvern, Pennsylvania). The mice bearing A431 tumors (for each group n = 4) were injected with Al^{18}F-NOTA-$Z_{EGFR:1907}$ (1.9−2.6 MBq) or ^{18}F-CBT-$Z_{EGFR:1907}$ (1.48−2.22 MBq) spiked with 30 or 300 μg of nonradioactive Ac-Cys-$Z_{EGFR:1907}$ or Cys-$Z_{EGFR:1907}$ through the tail vein. At 1, 2, and 3 h after injection, the mice were anesthetized with 2% isoflurane and placed near the center of the field of view of the microPET scanner in prone position. Three-minute static scans were obtained, and the images were reconstructed by a two-dimensional ordered subsets expectation maximum (OSEM) algorithm. No background correction was performed. Regions of interest (ROIs; 5 pixels for coronal and transaxial slices) were drawn over the tumors on decay-corrected whole-body coronal images. The maximum counts per pixel per minute were obtained from the ROIs and converted to counts per milliliter per minute using a calibration constant. Tissue density was assumed to be 1 g/mL, and the ROIs were converted to counts per gram per minute. Image ROI-derived %ID/g values were determined by dividing counts per gram per minute by the injected dose. No attenuation correction was performed.

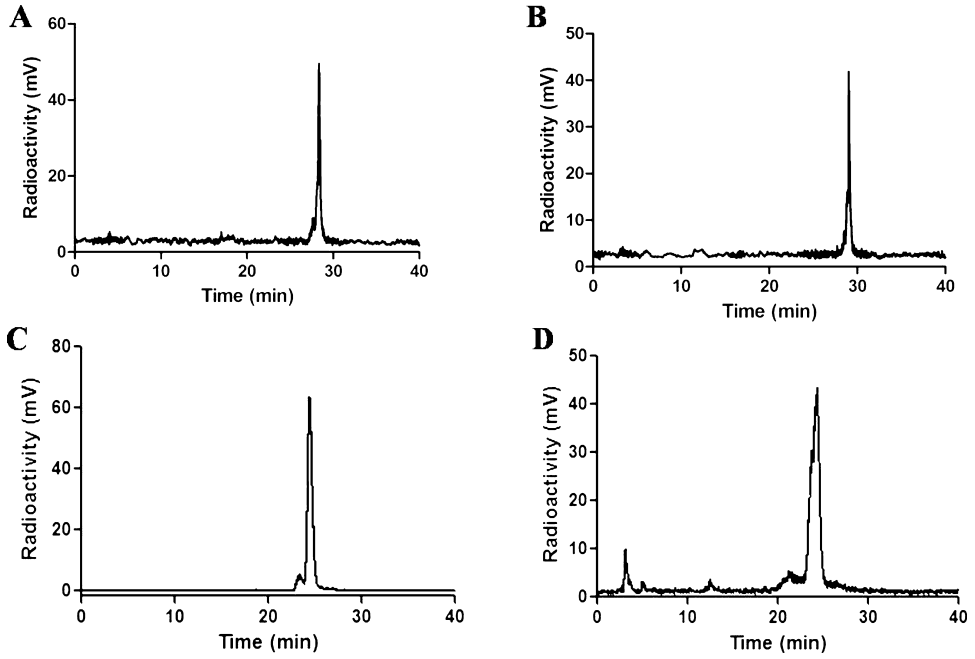

Figure 2. *In vitro* stability assay of Al^{18}F-NOTA-Z$_{EGFR:1907}$ (A,B) and ^{18}F-CBT-Z$_{EGFR:1907}$ (C,D) after incubation in mouse serum for 1 h (A,C) and 2 h (B,D).

Statistical Methods. Statistical analysis was performed using Student's two-tailed *t*-test for unpaired data. A 95% confidence level was chosen to determine the significance between groups, with a *P* value less than 0.05 being indicated as a significant difference.

RESULTS

Chemistry and Radiochemistry. The affibody molecules Ac-Cys-Z$_{EGFR:1907}$ and Cys-Z$_{EGFR:1907}$ with a cysteine at the N-terminal were successfully synthesized using conventional solid phase peptide synthesis and purified by semipreparative HPLC. The peptides were generally obtained in 10% yield. The retention time for both on analytical HPLC was 26 min. The purified Ac-Cys-Z$_{EGFR:1907}$ and Cys-Z$_{EGFR:1907}$ were characterized by MALDI-TOF-MS. The measured molecular weights (MWs) for both constructs were consistent with the expected MWs (for Ac-Cys-Z$_{EGFR:1907}$, calculated MW = 6690.0 and found MW = 6690.7; for Cys-Z$_{EGFR:1907}$, calculated MW = 6646.0 and found MW = 6645.7). Ac-Cys-Z$_{EGFR:1907}$ was then conjugated with MMA-NOTA and purified by HPLC. The measured MW of the final product (NOTA-Z$_{EGFR:1907}$) was m/z = 7112.0 for $[M + H]^+$ (calculated $MW_{[M+H]^+}$ = 7112.6), and the purity of NOTA-Z$_{EGFR:1907}$ was over 95% (retention time = 29 min). Lastly, purified ^{19}F-NOTA-Z$_{EGFR:1907}$ and ^{19}F-CBT-Z$_{EGFR:1907}$ were also characterized by MALDI-TOF-MS. The measured MWs for both constructs were consistent with the expected MWs (for ^{19}F-NOTA-Z$_{EGFR:1907}$, calculated MW = 7256.0 and measured MW = 7256.6; for ^{19}F-CBT-Z$_{EGFR:1907}$, calculated MW = 6852.0 and measured MW = 6852.9). The recovery yields of ^{19}F-NOTA-Z$_{EGFR:1907}$ and ^{19}F-CBT-Z$_{EGFR:1907}$ were 70% and 85%, respectively, after purification (retention time, 29 and 26.4 min).

The whole radiosynthesis of ^{18}F-NOTA-Z$_{EGFR:1907}$ was accomplished within 40 min. For ^{18}F-CBT-Z$_{EGFR:1907}$, the total radiosynthesis was completed within 120 min. ^{18}F-NOTA-Z$_{EGFR:1907}$ and ^{18}F-CBT-Z$_{EGFR:1907}$ showed a retention time of 29 and 26.4 min on HPLC, respectively. Both products were found to be more than 95% radiochemically pure, as determined by analytic HPLC. The overall radiochemical yields with decay correction at the end of synthesis for Al^{18}F-NOTA-Z$_{EGFR:1907}$ and ^{18}F-CBT-Z$_{EGFR:1907}$ were 15% and 41%, respectively. The specific activity of Al^{18}F-NOTA-Z$_{EGFR:1907}$ and ^{18}F-CBT-Z$_{EGFR:1907}$ were approximately 1.5×10^3 and 22.2×10^3 MBq/μmol, respectively.

***In Vitro* Stability and Metabolite Analysis.** *In vitro* stability studies allowed us to observe that more than 90% of Al^{18}F-NOTA-Z$_{EGFR:1907}$ remained intact during 1 to 2 h of incubation in mouse serum (Figure 2A,B). More than 90% of ^{18}F-CBT-Z$_{EGFR:1907}$ remained intact after 1 h incubation in mouse serum, while there was about 75% intact ^{18}F-CBT-Z$_{EGFR:1907}$ after 2 h of incubation (Figure 2C,D). Next, the *in vivo* stability studies are shown in Figure 3. In plasma and tumor, 90% and 85%, respectively, of Al^{18}F-NOTA-Z$_{EGFR:1907}$ remained intact (Figure 3A,B) at 1 h after injection, indicating excellent stability *in vivo*. However, ^{18}F-CBT-Z$_{EGFR:1907}$ showed much faster degradation *in vivo*, with only 40% and 24% of intact tracer product in plasma and tumor, respectively (Figure 3C,D).

***In Vitro* Cell Binding Assays.** Cell uptake levels for Al^{18}F-NOTA-Z$_{EGFR:1907}$ and ^{18}F-CBT-Z$_{EGFR:1907}$ are shown in Figure 4A,C, respectively. Al^{18}F-NOTA-Z$_{EGFR:1907}$ quickly accumulated in A431 cells and reached a highest value of 12% of applied activity at 1 h. A similar cell uptake pattern was observed for ^{18}F-CBT-Z$_{EGFR:1907}$, but the uptake level was much lower than that observed for Al^{18}F-NOTA-Z$_{EGFR:1907}$ at 1 h (7% of applied activity). When both probes were incubated with large excesses of nonradioactive affibody molecules (Ac-Cys-Z$_{EGFR:1907}$ or Cys-Z$_{EGFR:1907}$), their uptake levels in A431 cells were significantly inhibited ($P < 0.05$) at all incubation time points (Figure 4A,C).

The binding affinity of Al^{18}F-NOTA-Z$_{EGFR:1907}$ and ^{18}F-CBT-Z$_{EGFR:1907}$ to EGFR was determined through the receptor saturation assay. As shown in Figure 4B,D, the mean ± SD of K_D values of Al^{18}F-NOTA-Z$_{EGFR:1907}$ and ^{18}F-CBT-Z$_{EGFR:1907}$ were 12.72 ± 1.25 and 25.82 ± 3.62 nM, respectively. Al^{18}F-NOTA-Z$_{EGFR:1907}$ showed a lower K_D value compared to ^{18}F-CBT-Z$_{EGFR:1907}$. Overall, these results strongly suggested that PET probes Al^{18}F-NOTA-Z$_{EGFR:1907}$ and ^{18}F-CBT-Z$_{EGFR:1907}$ had high

dx.doi.org/10.1021/mp5003043 | *Mol. Pharmaceutics* 2014, 11, 3947−3956

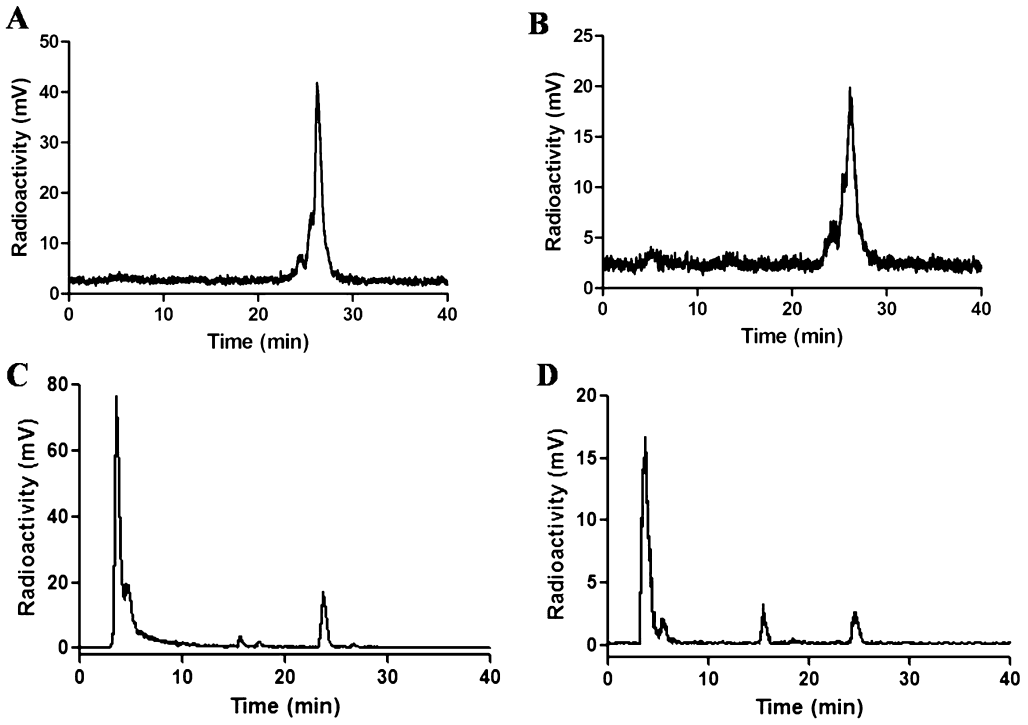

Figure 3. *In vivo* stability assay of $Al^{18}F$-NOTA-$Z_{EGFR:1907}$ (A,B) and ^{18}F-CBT-$Z_{EGFR:1907}$ (C,D) from samples of plasma (A,C) and tumor (B,D) at 1 h after injection.

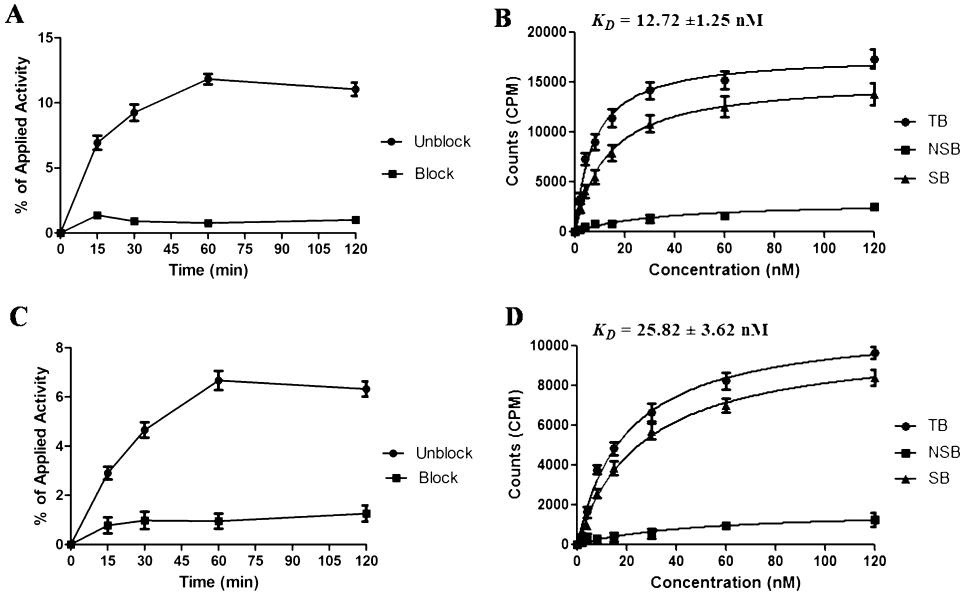

Figure 4. Characterization of EGFR-specific binding. (A,C) Cell uptakes of $Al^{18}F$-NOTA-$Z_{EGFR:1907}$ (A) and ^{18}F-CBT-$Z_{EGFR:1907}$ (C) in A431 cells over time at 37 °C with or without the presence of nonradioactive affibody molecules Ac-Cys-$Z_{EGFR:1907}$ or Cys-$Z_{EGFR:1907}$. (B,D) Saturation assay of $Al^{18}F$-NOTA-$Z_{EGFR:1907}$ (B) and ^{18}F-CBT-$Z_{EGFR:1907}$ (D) using A431 cells plotted by the concentration of total radioligands versus bound radioligand. NSB, nonspecific binding; TB, total binding; and SB, specific binding. All results are expressed as the mean of triplicate measurements ± standard deviation.

EGFR-binding specificity and affinity, which warranted their further evaluation *in vivo*.

***In Vivo* Biodistribution Studies.** At 3 h after injection, the biodistribution profiles of $Al^{18}F$-NOTA-$Z_{EGFR:1907}$ and ^{18}F-CBT-$Z_{EGFR:1907}$ are presented in Table 1. Both ^{18}F-labeled affibody molecules displayed relatively high levels of radioactivity accumulation in A431 tumors (4.77 ± 0.36 and 4.08 ± 0.54 % ID/g for $Al^{18}F$-NOTA-$Z_{EGFR:1907}$ and ^{18}F-CBT-$Z_{EGFR:1907}$, respectively). The value of tumor uptake for $Al^{18}F$-NOTA-$Z_{EGFR:1907}$ was higher than that of ^{18}F-CBT-$Z_{EGFR:1907}$. $Al^{18}F$-NOTA-$Z_{EGFR:1907}$ also exhibited significantly higher kidney and liver uptake than ^{18}F-CBT-$Z_{EGFR:1907}$ (112.26 ± 12.57, 13.31 ± 0.80 and 8.12 ± 1.0, 3.08 ± 0.15 %ID/g, respectively, $P < 0.05$). Conversely, bone uptake of $Al^{18}F$-NOTA-$Z_{EGFR:1907}$ was significantly lower than that of ^{18}F-CBT-$Z_{EGFR:1907}$ (1.75 ± 0.35 and 12.99 ± 2.37 %ID/g, respectively, $P < 0.05$). Interestingly, most other organ uptakes of ^{18}F-CBT-$Z_{EGFR:1907}$, such as blood, heart, lungs, spleen, pancreas, stomach, brain, intestine, skin, and muscle, were higher

dx.doi.org/10.1021/mp5003043 | *Mol. Pharmaceutics* 2014, 11, 3947−3956

Table 1. Biodistribution Results for $Al^{18}F$-NOTA-$Z_{EGFR:1907}$ and ^{18}F-CBT-$Z_{EGFR:1907}$ in A431 Xenografts[a]

organ (%ID/g)	$Al^{18}F$-NOTA-$Z_{EGFR:1907}$ (3 h)		^{18}F-CBT-$Z_{EGFR:1907}$ (3 h)	
(spiked dose)	30 μg spike	300 μg (blocking)	30 μg spike	300 μg (blocking)
blood	2.36 ± 0.53[b]	1.18 ± 0.10[b,e]	2.90 ± 0.60[c]	1.83 ± 0.24[c,e]
heart	1.88 ± 0.29[b]	1.14 ± 0.27[b,e]	2.76 ± 0.21[c]	1.81 ± 0.26[c,e]
lungs	1.27 ± 0.48[b]	0.56 ± 0.25[b]	1.43 ± 0.41	0.65 ± 0.19
liver	13.31 ± 0.80[b,d]	3.34 ± 0.37[b,e]	3.08 ± 0.15[c,d]	2.01 ± 0.45[c,e]
spleen	1.65 ± 0.51	0.89 ± 0.24	2.52 ± 0.33[c]	1.54 ± 0.28[c]
pancreas	1.54 ± 0.20[b]	0.83 ± 0.43[b]	2.45 ± 0.38[c]	1.46 ± 0.15[c]
stomach	1.65 ± 0.12[b]	0.77 ± 0.12[b,e]	2.10 ± 0.37	1.36 ± 0.34[e]
brain	0.31 ± 0.05[b,d]	0.16 ± 0.05[b,e]	2.14 ± 0.37[c,d]	1.06 ± 0.47[c,e]
intestine	1.40 ± 0.38[b]	0.70 ± 0.18[b]	2.78 ± 0.71[c]	1.32 ± 0.09[c]
kidneys	112.27 ± 12.57[d]	104.00 ± 15.58[e]	8.12 ± 1.00[cd]	4.26 ± 0.96[ce]
skin	1.54 ± 0.32[b]	0.73 ± 0.25[b]	1.83 ± 0.18[c]	1.05 ± 0.11[c]
muscle	1.84 ± 0.28[b]	0.75 ± 0.26[b]	2.02 ± 0.31[c]	1.10 ± 0.30[c]
bone	1.75 ± 0.35[d]	1.27 ± 0.27[e]	12.99 ± 2.37[c,d]	5.45 ± 0.90[c,e]
tumor	4.77 ± 0.36[b]	1.78 ± 0.30[b]	4.08 ± 0.54[c]	2.34 ± 0.21[c]
uptake ratio tumor to blood	2.08 ± 0.34	1.52 ± 0.27	1.44 ± 0.29	1.31 ± 0.29
tumor to lung	4.17 ± 0.20	3.77 ± 0.62	3.0 ± 0.54	3.85 ± 0.50
tumor to muscle	2.62 ± 0.33	2.74 ± 0.78	2.06 ± 0.41	2.22 ± 0.47
tumor to liver	0.36 ± 0.02[b,d]	0.53 ± 0.06[b,e]	1.33 ± 0.20[d]	1.22 ± 0.32[e]
tumor to kidney	0.04 ± 0.005[b,d]	0.02 ± 0.004[b,e]	0.50 ± 0.55[d]	0.56 ± 0.01[e]
tumor to bone	2.81 ± 0.62[b,d]	1.47 ± 0.46[b,e]	0.32 ± 0.07[d]	0.44 ± 0.08[e]

[a]Data are mean ± SD, expressed as percentage administered activity (injected probe) per gram of tissue (%ID/g) after intravenous injection of probe ($Al^{18}F$-NOTA-$Z_{EGFR:1907}$ or ^{18}F-CBT-$Z_{EGFR:1907}$) spiked with 30 and 300 μg of Ac-Cys-$Z_{EGFR:1907}$ or Cys-$Z_{EGFR:1907}$ at 3 h after injection. Significant inhibition of $Al^{18}F$-NOTA-$Z_{EGFR:1907}$ or ^{18}F-CBT-$Z_{EGFR:1907}$ uptake was observed in A431 tumor of the blocked group (300 μg) ($P < 0.05$). Student's unpaired two tailed *t*-test was conducted. $P < 0.05$ was considered significant (for each group, $n = 4$). [b]$P < 0.05$, comparing 30 μg spike and 300 μg (blocking) of dose tracer biodistribution at 3 h after injection with $Al^{18}F$-NOTA-$Z_{EGFR:1907}$. [c]$P < 0.05$, comparing 30 μg spike and 300 μg (blocking) of dose tracer biodistribution at 3 h after injection with ^{18}F-CBT-$Z_{EGFR:1907}$. [d]$P < 0.05$, comparing 30 μg of spike tracer biodistribution of $Al^{18}F$-NOTA-$Z_{EGFR:1907}$ and ^{18}F-CBT-$Z_{EGFR:1907}$ at 3 h after injection. [e]$P < 0.05$, comparing 300 μg (blocking) of spike tracer biodistribution of $Al^{18}F$-NOTA-$Z_{EGFR:1907}$ and ^{18}F-CBT-$Z_{EGFR:1907}$ at 3 h after injection.

than those of $Al^{18}F$-NOTA-$Z_{EGFR:1907}$. Accordingly, $Al^{18}F$-NOTA-$Z_{EGFR:1907}$ provided higher tumor-to-blood, tumor-to-lung, tumor-to-muscle, and tumor-to-bone ratios than ^{18}F-CBT-$Z_{EGFR:1907}$, except for tumor-to-liver and tumor-to-kidney ratios (Table 1).

For the *in vivo* blocking study, coinjection of an excess (300 μg) of unlabeled Ac-Cys-$Z_{EGFR:1907}$ or Cys-$Z_{EGFR:1907}$ resulted in significant ($P < 0.05$) reduction in tumor uptake to 1.78 ± 0.33 and 2.34 ± 0.21 %ID/g for $Al^{18}F$-NOTA-$Z_{EGFR:1907}$ and ^{18}F-CBT-$Z_{EGFR:1907}$, respectively. Liver uptake also significantly ($P < 0.05$) decreased to 3.34 ± 0.37 and 2.01 ± 0.45 %ID/g for $Al^{18}F$-NOTA-$Z_{EGFR:1907}$ and ^{18}F-CBT-Z_{EGFR}, respectively. For ^{18}F-CBT-$Z_{EGFR:1907}$, kidney uptake also significantly decreased from 8.12 ± 1.0 to 4.26 ± 0.96 %ID/g ($P < 0.05$). However, for $Al^{18}F$-NOTA-$Z_{EGFR:1907}$, kidney uptake did not significantly change in the blocking group (112.27 ± 12.57 vs 104.0 ± 15.58 %ID/g, $P > 0.05$).

Small-Animal PET Imaging. PET images acquired at 1, 2, and 3 h after injection are shown in Figure 5. $Al^{18}F$-NOTA-$Z_{EGFR:1907}$ and ^{18}F-CBT-$Z_{EGFR:1907}$ both clearly visualized EGFR-expressing A431 xenografts. $Al^{18}F$-NOTA-$Z_{EGFR:1907}$ showed better tumor-to-background contrast and high levels of radioactivity accumulation in the kidneys and liver in comparison with ^{18}F-CBT-$Z_{EGFR:1907}$. However, bone uptake was higher for ^{18}F-CBT-$Z_{EGFR:1907}$ than that for $Al^{18}F$-NOTA-$Z_{EGFR:1907}$.

The activity accumulation of $Al^{18}F$-NOTA-$Z_{EGFR:1907}$ and ^{18}F-CBT-$Z_{EGFR:1907}$ in the A431 tumors and other organs was also quantified (Figure 6). Time−activity curves for the tumor and the contralateral muscle tissue are shown in Figure 7. The results showed higher tumor uptake and lower uptake in the other organs, except for the liver and kidneys, for $Al^{18}F$-NOTA-$Z_{EGFR:1907}$ when compared to ^{18}F-CBT-$Z_{EGFR:1907}$ at 1−3 h after injection. The uptake values (%ID/g) of tumor and other organs obtained from PET image data at 3 h after injection were consistent with the findings in the biodistribution studies. Moreover, when the probes were coinjected with 300 μg unlabeled Ac-Cys-$Z_{EGFR:1907}$ or Cys-$Z_{EGFR:1907}$, the tumor was barely visible on PET images at 1−3 h after injection both for $Al^{18}F$-NOTA-$Z_{EGFR:1907}$ and ^{18}F-CBT-$Z_{EGFR:1907}$ (Figure 5). A quantitative analysis of the PET images showed significantly ($P < 0.05$) lower tumor uptake for mice injected with 300 μg blocking dose when compared to a 30 μg spiking dose at all time points for both probes (Figure 6).

DISCUSSION

EGFR-targeted PET imaging is a promising tool to provide a real-time assay of EGFR expression in all tumor sites (primary and metastatic lesions) in living subjects. EGFR-targeted PET probes could not only be used for early detection of EGFR positive tumor recurrence and stratification of cancer patients but also for dose optimization of EGFR targeted therapy and monitoring the efficacy of EGFR-based tumor treatment. Preclinical literature data suggests that radiolabeled affibody molecules have superior imaging properties and higher sensitivity to detect EGFR in comparison with monoclonal antibodies and their fragments due to their small size (7 kDa), as well as excellent tumor targeting and retention, and rapid blood clearance.[8] Furthermore, ^{18}F, the most commonly used PET radionuclide, is widely available and presents almost ideal imaging properties, making this radionuclide highly clinically relevant. Combining the aforementioned optimal clinical characteristics to develop an imaging agent is significantly

dx.doi.org/10.1021/mp5003043 | *Mol. Pharmaceutics* 2014, 11, 3947−3956

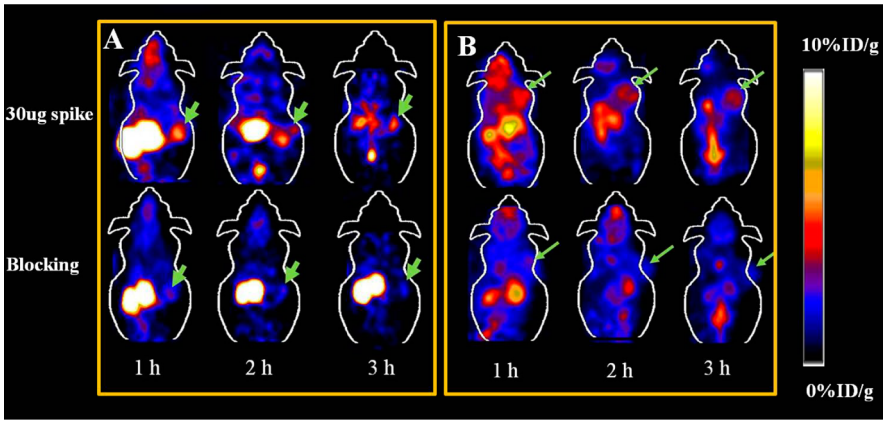

Figure 5. Decay-corrected coronal small-animal PET images of nude mice bearing A431 tumors at 1, 2, and 3 h after tail vein injection of Al^{18}F-NOTA-$Z_{EGFR:1907}$ (A) and ^{18}F-CBT-$Z_{EGFR:1907}$ (B) spiked with 30 μg (spike) and 300 μg (blocking) of cold affibody (Ac-Cys-$Z_{EGFR:1907}$ or Cys-$Z_{EGFR:1907}$, respectively). Arrows indicate the location of tumors (for each group, n = 4).

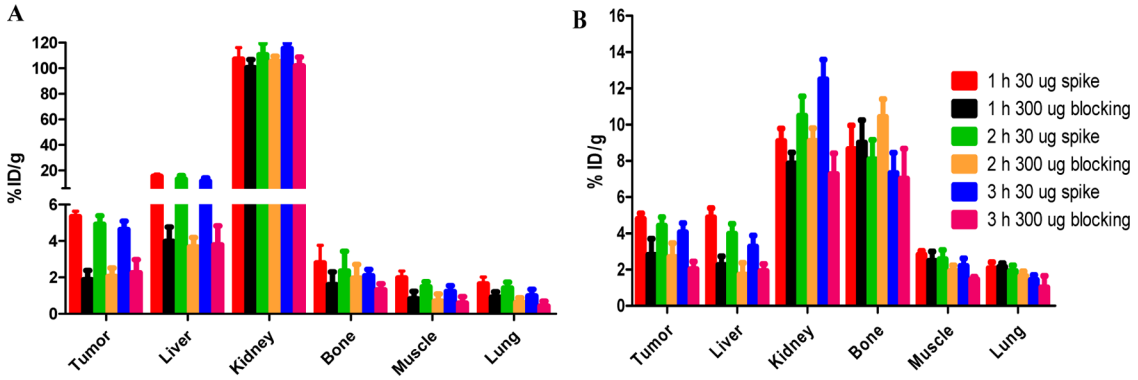

Figure 6. PET quantification analysis for uptakes of tumor, liver, kidney, bone, muscle, and lungs for Al^{18}F-NOTA-$Z_{EGFR:1907}$ (A) and ^{18}F-CBT-$Z_{EGFR:1907}$ (B) in A431 xenograft mice models after coinjection of with 30 μg (spike) or 300 μg (blocking) of cold affibody (Ac-Cys-$Z_{EGFR:1907}$ or Cys-$Z_{EGFR:1907}$, respectively) at 1, 2, and 3 h after injection. ROI was drawn on coronal images. Uptake was calculated with the mean uptake value (for each group, n = 4).

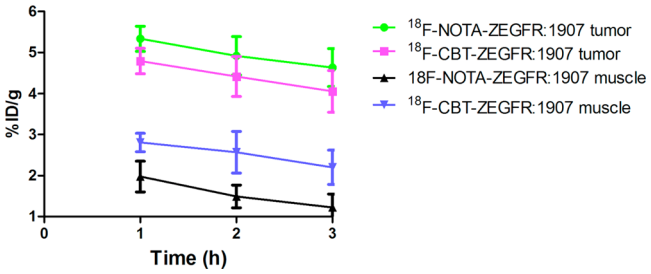

Figure 7. Tumor and muscle time−activity curves derived from multiple-time-point small-animal PET images in A431 xenograft mice models after coinjection of Al^{18}F-NOTA-$Z_{EGFR:1907}$ or ^{18}F-CBT-$Z_{EGFR:1907}$ with 30 μg (spike) of cold affibody (Ac-Cys-$Z_{EGFR:1907}$ or Cys-Z $_{EGFR:1907}$, respectively) at 1, 2, and 3 h after injection. Data are shown as mean ± SD %ID/g (n = 4).

important since our goal is to ultimately apply affibody-based PET probes for imaging patients.

We have previously developed an ^{18}F labeled affibody molecule $Z_{EGFR:1907}$ (^{18}F-FBEM-$Z_{EGFR:1907}$).[12] However, the ^{18}F labeling strategies used in that work involved lengthy (3 h) and tedious multistep radiosynthetic procedures. Moreover, it is very challenging to adapt these radiosynthetic processes into a fully automated radiosynthetic platform, which creates a considerable technical barrier for using these affibody-based PET probes in the clinical setting. Very recently, we have successfully used two methods for RGD peptide radiofluorination (^{18}F-AlF-NOTA and ^{18}F-CBT) in no more than two radiosynthetic steps within 40 and 120 min, respectively.[16,18] These recently described strategies provide straightforward, quicker, and powerful ^{18}F labeling methods to radiofluorinate biomolecules for *in vivo* molecular imaging applications.

In the present study, only a 1-pot reaction was involved in the procedures to obtain Al^{18}F-NOTA-$Z_{EGFR:1907}$ in a total preparation time of 40 min, with a decay-corrected yield at the end of synthesis of 15%. For ^{18}F-CBT-$Z_{EGFR:1907}$, 2-pot reactions and 2 h were required in the radiosynthesis with a yield of 41%. Compared with the radiosynthesis of ^{18}F-FBEM-$Z_{EGFR:1907}$, Al^{18}F-NOTA-$Z_{EGFR:1907}$ and ^{18}F-CBT-$Z_{EGFR:1907}$ were superior to ^{18}F-FBEM-$Z_{EGFR:1907}$ (3 h preparation time and 10% radiochemical yield). However, both radiochemical yields were less than those previously described for the ^{18}F-labeled peptides Al^{18}F-NOTA-RGD_2 (17.9%)[18] and ^{18}F-CBT-RGD_2 (80%).[16] It is likely that the lower radiochemical yields observed were due to the fact that the concentration of the affibody molecules (Ac-Cys-$Z_{EGFrefR:1907}$ or Cys-$Z_{EGFR:1907}$; 0.84 or 0.11 mmol/L) was much lower than that of the peptides RGD_2 (36.6 or 3.55 mmol/L). Further optimization of our current labeling procedure is under investigation and may result in a higher radiolabeling yield of Al^{18}F-NOTA-$Z_{EGFR:1907}$ and ^{18}F-CBT-$Z_{EGFR:1907}$ by modifying synthetic environment (pH or temperature). Nonetheless, our study demonstrates that both Al^{18}F-NOTA

dx.doi.org/10.1021/mp5003043 | *Mol. Pharmaceutics* 2014, 11, 3947−3956

and ^{18}F-CBT can be used for ^{18}F labeling of small proteins and have high potential for generating PET probes for different applications. Moreover, the stability studies reveal that Al^{18}F-NOTA-$Z_{EGFR:1907}$ is highly stable *in vitro* and *in vivo*, whereas the *in vivo* stability of ^{18}F-CBT-$Z_{EGFR:1907}$ is not ideal and requires further improvement.

The biologic properties of Al^{18}F-NOTA-$Z_{EGFR:1907}$ and ^{18}F-CBT-$Z_{EGFR:1907}$ were evaluated by *in vitro* cell assays, biodistribution studies, and small-animal PET imaging studies. Both Al^{18}F-NOTA-$Z_{EGFR:1907}$ and ^{18}F-CBT-$Z_{EGFR:1907}$ showed significantly high uptake in A431 cells, demonstrating their EGFR-binding specificity *in vitro*. ^{18}F-CBT-$Z_{EGFR:1907}$ showed lower cell uptake than Al^{18}F-NOTA-$Z_{EGFR:1907}$. This result was likely caused by the higher EGFR-binding affinity of Al^{18}F-NOTA-$Z_{EGFR:1907}$ (25.82 ± 3.62 vs 12.72 ± 1.25 nM). Compared with ^{18}F-FBEM-$Z_{EGFR:1907}$ (K_D = 37 ± 3.0 nM), Al^{18}F-NOTA-$Z_{EGFR:1907}$ and ^{18}F-CBT-$Z_{EGFR:1907}$ both showed high binding affinity with a K_D of 12.72 ± 1.25 and 25.82 ± 3.62 nM, respectively.

It is known that the high natural expression of EGFR in the liver creates a biological barrier to radioprobes targeting the EGFR positive tumors by reducing tumor uptake.[20] Saturating the EGFR in the liver can increase tumor uptake of EGFR targeted probes. Our previous study demonstrated that improved imaging contrasts of EGFR positive tumor can be achieved with optimized spiking doses (5−50 μg) along with the injection of ^{64}Cu-DOTA-$Z_{EGFR:1907}$.[13] Therefore, for both Al^{18}F-NOTA-$Z_{EGFR:1907}$ and ^{18}F-CBT-$Z_{EGFR:1907}$, spiking doses of cold Z_{EGFR} were used directly for *in vivo* evaluation. After evaluating two probes in mice, it was found that Al^{18}F-NOTA-$Z_{EGFR:1907}$ shows some advantages over ^{18}F-CBT-$Z_{EGFR:1907}$ as a promising agent for EGFR imaging. Al^{18}F-NOTA-$Z_{EGFR:1907}$ rapidly localizes in A431 tumors and shows good tumor uptake, retention, and tumor-to-muscle ratios, allowing clear visualization of A431 tumors by PET at even 1 h postinjection. The highest uptake observed in the kidneys and the liver is mainly attributed to the fact that they are the major organs responsible for metabolism and clearance. High kidney uptake could be associated with radiolabeled affibody molecules being reabsorbed by the organ. Additionally, liver uptake might be increased due to the fact that this organ also highly expresses EGFR.[12] The *in vivo* EGFR-binding specificity of Al^{18}F-NOTA-$Z_{EGFR:1907}$ was also confirmed by the reduced A431 tumor and liver uptake observed after coinjection with 300 μg of Ac-Cys-$Z_{EGFR:1907}$. Moreover, low radioactivity levels were found in the lung, intestine, spleen, and stomach. The low uptake of Al^{18}F-NOTA-$Z_{EGFR:1907}$ in these normal organs makes the PET probe a potential agent to detect primary or metastatic tumors expressing EGFR in the abdomen and lung region. Only low activity was observed in the brain, suggesting that Al^{18}F-NOTA-$Z_{EGFR:1907}$ cannot penetrate through the blood−brain barrier. Interestingly, the kidney uptake of Al^{18}F-NOTA-$Z_{EGFR:1907}$ was not reduced by the unlabeled affibody at all the time points, whereas ^{18}F-CBT-$Z_{EGFR:1907}$ was moderately blocked at late time point (3 h) but not at early time points (1 and 2 h). These data suggest the kidney uptake of two probes is not likely receptor mediated. The blocking effort for ^{18}F-CBT-$Z_{EGFR:1907}$ at 3 h *p.i.* may be somewhat linked to the *in vivo* instability of ^{18}F-CBT-$Z_{EGFR:1907}$. Further studies are required to reveal the observations. Overall, these results indicate that Al^{18}F-NOTA-$Z_{EGFR:1907}$ is characterized by a relatively easy preparation, favorable pharmacokinetic properties, and high specificity for EGFR, which render it a useful agent for *in vivo* imaging of EGFR positive tumors and related applications.

In contrast, the performance of ^{18}F-CBT-$Z_{EGFR:1907}$ *in vivo* was not ideal: relatively high uptake in most normal tissues (such as brain, pancreas, spleen, intestine, blood, muscle, lung, and spleen), especially the remarkably high uptake in bone (13.0 ± 2.37 %ID/g), suggests *in vivo* release of ^{18}F-fluoride (Table 1). In fact, bone uptake of ^{18}F-CBT-$Z_{EGFR:1907}$ was about 3-fold higher than that observed for Al^{18}F-NOTA-$Z_{EGFR:1907}$. Also, the *in vitro* stability and metabolite analysis studies, where only about 75%, 40%, and 24% of ^{18}F-CBT-$Z_{EGFR:1907}$ was intact after 2 h of serum incubation or in plasma and tumor *in vivo* at 1 h after injection, suggest that ^{18}F-CBT-$Z_{EGFR:1907}$ is not stable *in vivo*. The kidney and the liver showed the lowest uptake (8.12 ± 1.0 and 3.08 ± 0.15 %ID/g) at 3 h after injection. These results are in agreement with our previous data[17] indicating that polar metabolites clear more rapidly from blood.

NOTA has already been coupled to affibody molecules ($Z_{HER2:2395}$ and $Z_{HER2:S1}$) and the conjugates radiolabeled with ^{111}In, ^{68}Ga, and ^{18}F for HER2 imaging.[17,21] Our data are generally consistent with the findings reported in these published studies. For example, it was reported that Al^{18}F-NOTA-$Z_{HER2:2395}$ displayed uptake of 4.4 ± 0.8 and 4.9 ± 0.7 %ID/g in SKOV3 tumors at 1 and 4 h after injection, respectively, whereas the corresponding levels in the kidneys were high (about 140 and 150 %ID/g, from Figure 3) and in the bone low (1 %ID/g, from Figure 3).[17] In the present study, the uptake of Al^{18}F-NOTA-$Z_{EGFR:1907}$ in A431 tumors at 3 h after injection were 4.77 ± 0.34 %ID/g, and the corresponding levels in kidney and bone were 112.27 ± 12.57 and 1.75 ± 0.35 %ID/g, respectively. Overall, Al^{18}F-NOTA radiolabeled affibody molecules rapidly accumulated in tumors, with high uptake and good tumor-to-normal tissue ratios and low uptake in the bone indicating stable complexation in the form of Al^{18}F by the NOTA chelator. However, they typically showed high uptake in the kidneys as well, probably because radiolabeled affibody molecules were excreted and reabsorbed by the kidneys. In order to minimize the reabsorption of affibody molecules by the kidneys, the pharmacokinetics could be further improved with strategies such as the use of positively charged amino acids, gelofusin, or albumin fragments.[22−24] Moreover, compared with ^{18}F-FBEM-$Z_{EGFR:1907}$,[12] Al^{18}F-NOTA-$Z_{EGFR:1907}$ had a lower tumor uptake (4.77 ± 0.36 vs 8.06 ± 1.44 %ID/g) at 3 h after injection, probably due to the effect of different ^{18}F-radiolabeling group. In our previous study,[16] we had also successfully developed ^{18}F-CBT-RGD_2 and ^{18}F-CBT-RLuc. Both probes demonstrated high levels of tumor accumulation and favorable pharmacokinetic properties. However, in the present study, it has been found that ^{18}F-CBT-$Z_{EGFR:1907}$ was degraded *in vivo*. Therefore, great efforts will be focused on introducing appropriate molecular modifications, such as the use of more stable D-amino acids for L-amino acids, the use of pseudopeptide bonds,[25] modifying synthetic environment, etc.

CONCLUSIONS

Two strategies for ^{18}F-labeling affibody molecules have been successfully developed with either NOTA or CBT coupling to affibody molecules that contain an N-terminal cysteine as two model platforms. These two methods can potentially be translated to other applications. High activities of the probes can be reliably obtained in a relatively short radiosynthesis time. Biodistribution and small-animal PET imaging studies demonstrated that Al^{18}F-NOTA-$Z_{EGFR:1907}$ is a promising PET probe for imaging EGFR expression in living mice. In contrast, ^{18}F-CBT-$Z_{EGFR:1907}$ may be easily degraded *in vivo* compared to Al^{18}F-NOTA-$Z_{EGFR:1907}$. Further research is needed to improve the

stability of ^{18}F-CBT-$Z_{EGFR:1907}$ *in vivo* and determine whether this probe can be used for patient EGFR PET imaging.

AUTHOR INFORMATION

Corresponding Author

*(Z.C.) Phone: 650-723-7866. Fax: 650-736-7925. E-mail: zcheng@stanford.edu.

Notes

The authors declare no competing financial interest.

ACKNOWLEDGMENTS

We thank Yang Liu, Hongguang Liu, Shuxiang Meng, Jibo Li, Chunxia Qin, Zheng Miao, and Morten Persson for technical assistance. This research was partially supported by the Office of Science (BER), U.S. Department of Energy (DE-SC0008397), *In vivo* Cellular Molecular Imaging Center (ICMIC) grant P50 CA114747, National Natural Science Foundation of China (81071182), and Medical Innovation Foundation of Fujian, China (2009-CXB-46).

REFERENCES

(1) Mendelsohn, J.; Baselga, J. Epidermal growth factor receptor targeting in cancer. *Semin. Oncol.* **2006**, *33* (4), 369−385.

(2) Chen, S. J.; Luan, J.; Zhang, H. S.; Ruan, C. P.; Xu, X. Y.; Li, Q. Q.; Wang, N. H. EGFR-mediated G1/S transition contributes to the multidrug resistance in breast cancer cells. *Mol. Biol. Rep.* **2012**, *39* (5), 5465−5471.

(3) Hoffmann, K.; Xiao, Z.; Franz, C.; Mohr, E.; Serba, S.; Büchler, M. W.; Schemmer, P. Involvement of the epidermal growth factor receptor in the modulation of multidrug resistance in human hepatocellular carcinoma cells in vitro. *Cancer Cell Int.* **2011**, *11*, 40.

(4) Liang, K.; Ang, K. K.; Milas, L.; Hunter, N.; Fan, Z. The epidermal growth factor receptor mediates radioresistance. *Int. J. Radiat. Oncol. Biol. Phys.* **2003**, *57* (1), 246−254.

(5) Pantaleo, M. A.; Nannini, M.; Maleddu, A.; Fanti, S.; Nanni, C.; Boschi, S.; Lodi, F.; Nicoletti, G.; Landuzzi, L.; Lollini, P. L.; Biasco, G. Experimental results and related clinical implications of PET detection of epidermal growth factor receptor (EGFr) in cancer. *Ann. Oncol.* **2009**, *20* (2), 213−226.

(6) Friedman, M.; Nordberg, E.; Höidén-Guthenberg, I.; Brismar, H.; Adams, G. P.; Nilsson, F. Y.; Carlsson, J.; Stahl, S. Phage display selection of affibody molecules with specific binding to the extracellular domain of the epidermal growth factor receptor. *Protein Eng. Des. Sel.* **2007**, *20* (4), 189−199.

(7) Cheng, Z.; De Jesus, O. P.; Kramer, D. J.; De, A.; Webster, J. M.; Gheysens, O.; Levi, J.; Namavari, M.; Wang, S.; Park, J. M.; Zhang, R.; Liu, H.; Lee, B.; Syud, F. A.; Gambhir, S. S. 64Cu-labeled affibody molecules for imaging of HER2 expressing tumors. *Mol. Imaging Biol.* **2010**, *12* (3), 316−324.

(8) Cheng, Z.; De Jesus, O. P.; Namavari, M.; De, A.; Levi, J.; Webster, J. M.; Zhang, R.; Lee, B.; Syud, F. A.; Gambhir, S. S. Small-animal PET imaging of human epidermal growth factor receptor type 2 expression with site-specific 18F-labeled protein scaffold molecules. *J. Nucl. Med.* **2008**, *49* (5), 804−813.

(9) Ren, G.; Zhang, R.; Liu, Z.; Webster, J. M.; Miao, Z.; Gambhir, S. S.; Syud, F. A.; Cheng, Z. A 2-helix small protein labeled with 68Ga for PET imaging of HER2 expression. *J. Nucl. Med.* **2009**, *50* (9), 1492−1499.

(10) Webster, J. M.; Zhang, R.; Gambhir, S. S.; Cheng, Z.; Syud, F. A. Engineered two-helix small proteins for molecular recognition. *ChemBioChem* **2009**, *10* (8), 1293−1296.

(11) Baum, R. P.; Prasad, V.; Müller, D.; Schuchardt, C.; Orlova, A.; Wennborg, A.; Tolmachev, V.; Feldwisch, J. Molecular imaging of HER2-expressing malignant tumors in breast cancer patient using synthetic 111In- or 68Ga-labeled affibody molecules. *J. Nucl. Med. Med.* **2010**, *51* (6), 892−897.

(12) Miao, Z.; Ren, G.; Liu, H.; Qi, S.; Wu, S.; Cheng, Z. PET of EGFR expression with an 18F-labeled affibody molecule. *J. Nucl. Med.* **2012**, *53* (7), 1110−1118.

(13) Miao, Z.; Ren, G.; Liu, H.; Jiang, L.; Cheng, Z. Small-animal PET imaging of human epidermal growth factor receptor positive tumor with a 64Cu labeled affibody protein. *Bioconjugate Chem.* **2010**, *21* (5), 947−954.

(14) McBride, W. J.; Sharkey, R. M.; Karacay, H.; D'Souza, C. A.; Rossi, E. A.; Laverman, P.; Chang, C. H.; Boerman, O. C.; Goldenberq, D. M. A novel method of 18F radiolabeling for PET. *J. Nucl. Med.* **2009**, *50* (6), 991−998.

(15) Laverman, P.; McBride, W. J.; Sharkey, R. M.; Eek, A.; Joosten, L.; Oyen, W. J.; Goldenberq, D. M.; Boerman, Q. C. A novel facile method of labeling octreotide with (18)F-fluorine. *J. Nucl. Med.* **2010**, *51* (3), 454−461.

(16) Jeon, J.; Shen, B.; Xiong, L.; Miao, Z.; Lee, K. H.; Rao, J.; Chin, F. T. Efficient method for site-specific 18F-labeling of biomolecules using the rapid condensation reaction between 2-cyanobenzothiazole and cysteine. *Bioconjugate Chem.* **2012**, *23* (9), 1902−1908.

(17) Heskamp, S.; Laverman, P.; Rosik, D.; Boschetti, F.; van der Graaf, W. T.; Oyen, W. J.; van Laarhoven, H. W.; Tolmachev, V.; Boerman, O. C. Imaging of human epidermal growth factor receptor type 2 expression with 18F-labeled affibody molecule ZHER2:2395 in a mouse model for ovarian cancer. *J. Nucl. Med.* **2012**, *53* (1), 146−153.

(18) Liu, S.; Liu, H.; Jiang, H.; Xu, Y.; Zhang, H.; Cheng, Z. One-step radiosynthesis of ^{18}F-AlF-NOTA-RGD_2 for tumor angiogenesis PET imaging. *Eur. J. Nucl. Med. Mol. Imaging* **2011**, *38* (9), 1732−1741.

(19) Wan, W.; Guo, N.; Pan, D.; Yu, C.; Weng, Y.; Luo, S.; Ding, H.; Xu, Y.; Wang, L.; Lang, L.; Xie, Q.; Yang, M.; Chen, X. First experience of 18F-alfatide in lung cancer patients using a new lyophilized kit for rapid radiofluorination. *J. Nucl. Med.* **2013**, *54* (5), 691−698.

(20) Kareem, H.; Sandström, K.; Elia, R.; Gedda, L.; Anniko, M.; Lundqvist, H.; Nestor, M. Blocking EGFR in the liver improves the tumor-to-liver uptake ratio of radiolabeled EGF. *Tumour Biol.* **2010**, *31* (2), 79−87.

(21) Malmberg, J.; Perols, A.; Varasteh, Z.; Altai, M.; Braun, A.; Sandström, M.; Garske, U.; Tolmachev, V.; Orlova, A.; Karlström, A. E. Comparative evaluation of synthetic anti-HER2 Affibody molecules site-specifically labelled with 111In using N-terminal DOTA, NOTA and NODAGA chelators in mice bearing prostate cancer xenografts. *Eur. J. Nucl. Med. Mol. Imaging* **2012**, *39* (3), 481−492.

(22) van Eerd, J. E.; Vegt, E.; Wetzels, J. F.; Russel, F. G.; Masereeuw, R.; Corstens, F. H.; Oyen, W. J.; Boerman, O. C. Gelatin-based plasma expander effectively reduces renal uptake of 111In-octreotide in mice and rats. *J. Nucl. Med.* **2006**, *47* (3), 528−533.

(23) Vegt, E.; van Eerd, J. E.; Eek, A.; Oyen, W. J.; Wetzels, J. F.; de Jong, M.; Russel, F. G.; Masereeuw, R.; Gotthardt, M.; Boerman, O. C. Reducing renal uptake of radiolabeled peptides using albumin fragments. *J. Nucl. Med.* **2008**, *49* (9), 1506−15 11.

(24) Rolleman, E. J.; Valkema, R.; de Jong, M.; Kooij, P. P.; Krenning, E. P. Safe and effective inhibition of renal uptake of radiolabelled octreotide by a combination of lysine and arginine. *Eur. J. Nucl. Med. Mol. Imaging* **2003**, *30* (1), 9−15.

(25) Fani, M.; Maecke, H. R.; Okarvi, S. M. Radiolabeled peptides: valuable tools for the detection and treatment of cancer. *Theranostics* **2012**, *2* (5), 481−501.